AIP Journal of Applied Physics

New insight into the microstructure and doping of unintentionally n-type microcrystalline silicon carbide

Manuel Pomaska, Florian Köhler, Uwe Zastrow, Jan Mock, Frank Pennartz, Stefan Muthmann, Oleksandr Astakhov, Reinhard Carius, Friedhelm Finger, and Kaining Ding

Citation: Journal of Applied Physics **119**, 175303 (2016); doi: 10.1063/1.4948479
View online: http://dx.doi.org/10.1063/1.4948479
View Table of Contents: http://scitation.aip.org/content/aip/journal/jap/119/17?ver=pdfcov
Published by the AIP Publishing

JOURNAL OF APPLIED PHYSICS **119**, 175303 (2016)

New insight into the microstructure and doping of unintentionally n-type microcrystalline silicon carbide

Manuel Pomaska,[a)] Florian Köhler, Uwe Zastrow, Jan Mock, Frank Pennartz, Stefan Muthmann, Oleksandr Astakhov, Reinhard Carius, Friedhelm Finger, and Kaining Ding

Forschungszentrum Jülich, IEK5-Photovoltaics, Wilhelm-Johnen-Strasse, 52425 Jülich, Germany

(Received 22 December 2015; accepted 20 April 2016; published online 6 May 2016)

Microcrystalline silicon carbide (μc-SiC:H) deposited by hot wire chemical vapor deposition (HWCVD) and plasma-enhanced chemical vapor deposition (PECVD) provide advantageous opto-electronic properties, making it attractive as a window layer material in silicon thin-film and silicon heterojunction solar cells. However, it is still not clear which electrical transport mechanisms yield dark conductivities up to 10^{-3} S/cm without the active use of any doping gas and how the transport mechanisms are related to the morphology of μc-SiC:H. To investigate these open questions systematically, we investigated HWCVD and PECVD grown layers that provide a very extensive range of dark conductivity values from 10^{-12} S/cm to 10^{-3} S/cm. We found out by secondary ion mass spectrometry measurements that no direct correlation exists between oxygen or nitrogen concentrations and high dark conductivity σ_d, high charge carrier density n, and low activation energy Ea. Higher σ_d seems to rise from lower hydrogen concentrations or/and larger coherent domain sizes L_{SiC}. On the one hand, the decrease of σ_d with increasing hydrogen concentration might be due to the inactivation of donors by hydrogen passivation that gives rise to decreased n. On the other hand, qualitatively consistent with the Seto model, the lower σ_d and lower n might be caused by smaller L_{SiC}, since the fraction of depleted grain boundaries with higher Ea increases accordingly. *Published by AIP Publishing.* [http://dx.doi.org/10.1063/1.4948479]

I. INTRODUCTION

Microcrystalline crystalline silicon carbide (μc-SiC:H) is a semiconductor material that is very suitable as a window layer in silicon-based thin-film solar cells[1,2] and silicon heterojunction solar cells,[3,4] due to the combination of wide band gap and high electrical conductivity. The deposition of μc-SiC:H using hot wire chemical vapor deposition (HWCVD)[5] or plasma-enhanced chemical vapor deposition (PECVD) has been described by several research groups in the past.[6,7] They reported on the n-type characteristic of the films, although no doping gas was actively added to a gas mixture of monomethylsilane (MMS) and molecular hydrogen. Nevertheless, intentional n-doping of μc-SiC:H with nitrogen[8] or phosphine[6] and intentional p-doping of μc-SiC:H by overcompensation with aluminum[9,10] or boron[11] are also possible. Although, the electrical conductivity of the material can be enhanced by several orders of magnitude by the active doping, the highest optical transparency is obtained in μc-SiC:H without any active doping. Therefore, we are interested in using this unintentionally n-doped μc-SiC:H as a window layer and in improving its electrical conductivity without any doping gas, which requires a better understanding of its electrical transport mechanisms.

To date, it is known that dark conductivity increases with higher crystalline volume fraction.[2,6] However, Köhler *et al.*[12] showed that the material is either crystalline or amorphous. Therefore, it is still unclear, how the structural properties of μc-SiC:H are related to the electrical properties. In order to perform a reliable and systematic study of the electrical properties of μc-SiC:H, a number of layers have been prepared with HWCVD and PECVD which cover a large range of dark conductivity, namely, from 1.0×10^{-12} to 3.0×10^{-3} S/cm. In this paper, we discuss the influence of stoichiometry, hydrogen (H) concentration, oxygen (O) and nitrogen (N) impurities, and silicon carbide (SiC) coherent domain size, on the electrical properties as dark conductivity (σ_d), charge carrier mobility (μ), charge carrier density (n), and activation energy (E_a) for HWCVD as well as for PECVD μc-SiC:H.

II. EXPERIMENTAL DETAILS

The μc-SiC:H layers were deposited either in a HWCVD vacuum chamber with three curled rhenium wires or in a PECVD vacuum chamber with an excitation frequency of 81.36 MHz. In both cases, we varied the flow rates of the MMS gas (F_{MMS}), which is diluted to 5% in H_2, from 2–20 sccm, and adapted an additional H_2 flow rate to keep the H_2 dilution at 99.7%. All other deposition parameters were kept constant. For HWCVD, the pressure was kept at 75 Pa, the heater temperature was 250 °C, and the filament temperature was 1950 °C. For PECVD, the pressure was kept at 100 Pa, the heater temperature was 450 °C, and the forward power was 120 W. All films were deposited on Corning glass (EAGLE XG) and p-type silicon wafer (100). Deposition time has been adjusted to achieve a thickness of

[a)]Author to whom correspondence should be addressed. Electronic mail: m.pomaska@fz-juelich.de. Telephone: +49 2461 61 96480. Fax: +49 2461 61 3735.

approximately 200 nm for all layers in the study. The thickness was measured by profilometer.

We derived an average cubic SiC coherent domain size (L_{SiC}) from X-ray diffraction (XRD) measurements by applying the Scherrer equation[13] on the 3C-SiC peak which involves peak position and full width at half maximum (FWHM). Fourier transform infrared (FTIR) measurements served as a comparison of the Si-C stretching mode with the XRD 3C-SiC peak and they further were used to determine the H concentration ([H]) quantitatively from the Si-H related modes, as reported by King *et al.*[14]

Secondary ion mass spectrometry (SIMS) depth profiling has been performed in UHV-ambient (residual gas pressure $<1 \times 10^{-10}$ mbar) with a quadrupol instrument (ATOMIKA 4000). In order to get better statistics and to rule out lateral deviation in the film composition, SIMS analysis of the μc-$Si_{1-x}C_x$:H(O,N) films has been repeated at least once at different areas of each sample. For depth profiling of oxygen ([O]) and nitrogen contaminations ([N]) within the μc-$Si_{1-x}C_x$ films, near-normal 6 keV Cs^+-bombardment and detection of negative secondary ions have been applied. The SIMS raw data have been quantified by relative sensitivity factors (RSFs), as determined via ^{16}O (dose $2 \times 10^{15}\,cm^{-2}$) and ^{14}N (dose $1 \times 10^{16}\,cm^{-2}$) ion implantations (150 keV ion acceleration in both cases) in single crystalline SiC-wafer.[15] Depth profiles of the silicon and carbon matrix elements have been collected during 6 keV Cs+-bombardment at 65°, with respect to the sample normal, applying the CsM+ technique.[16] The resulting 133Cs28Si+ and 133Cs12C+ dimer ion count rates have been quantified assuming constant sensitivity factors for both matrix species, as previously reported in the literature.[17,18] In case of the quantitative matrix elements analysis, the ratio of CsM+ sensitivity factors has been determined during sputter removal of single crystalline SiC wafer applying exactly the same bombardment conditions as used for depth profiling of the μc-$Si_{1-x}C_x$:H films, i.e., proceeding these calibration runs at least twice for each μc-SiC:H samples-set mounted on the SIMS sample holder.

Dark conductivity (σ_d) was measured at room temperature in atmosphere. Furthermore, temperature dependent measurements of σ_d and thermopower were performed over a coplanar contact distance of 4 mm in vacuum, as reported elsewhere.[19] Each data point of thermopower was determined by varying the temperature gradient from $\Delta T \approx +30$ K to -30 K. In this measurement, geometry, surface oxide layers, etc., do not play a role as long as they do not result in carrier accumulation within the material. We varied the temperature from 360 K to 600 K. Charge carrier density (n) was calculated from thermopower (S) using[20]

$$S = \frac{k_B}{q}\left[ln\left(\frac{N_C}{n}\right) + A_C\right], \qquad (1)$$

where k_B is the Boltzmann constant, q is the elementary charge, N_C is the effective density of states at the conduction band, and A_C is the heat of transport. Based on former investigations of μc-SiC:H(n): $N_C = 3 \times 10^{15}\,T^{3/2}$ and $A_C = 4$.[21] By using the results of n and σ_d, we also derived the charge carrier mobility (μ) with $\mu = \sigma_d/(qn)$. To determine the activation energy (E_a) we used the slope of σ_d in Arrhenius plot form at 360 K. From the slope of the Arrhenius plot of μ and n, we deduced the thermal activation of mobility (μ_T) and of charge carrier density (n_T). Because the thermopower setup requires an electrical resistance minor to 100 GΩ, not all samples could be measured. Thus, from our samples we could only measure layers with $\sigma_d \geq 10^{-9}$ S/cm.

III. RESULTS

In Fig. 1, σ_d and L_{SiC} are plotted as a function of F_{MMS}. The values for σ_d are very similar for both deposition methods. For HWCVD, σ_d decreased from 2.0×10^{-4} S/cm to 1×10^{-12} S/cm and, for PECVD, σ_d decreased from 7.6×10^{-4} S/cm to 1×10^{-11} S/cm with increasing F_{MMS}. For HWCVD and PECVD μc-SiC:H, L_{SiC} decreases with increasing F_{MMS}. For HWCVD-grown layers, L_{SiC} decreases from 49 nm to 0 nm and, for PECVD-grown layers, L_{SiC} decreases from 7 nm to 0 nm. The corresponding 3C-SiC XRD peaks are presented in Fig. 2. The 3C-SiC peak shifts for HWCVD from 35.63° to 35.33° and for PECVD from 35.22° to 34.65° with increasing F_{MMS}. Additionally, the FWHM of the 3C-SiC peak increases for HWCVD from 0.22297° to 0.22492° and for PECVD from 1.24° to 3.62° with increasing F_{MMS}.

In Fig. 3, the FTIR spectra of the layers deposited by HWCVD and PECVD μc-SiC:H layers are presented: the Si-C stretching mode at 770–800 cm^{-1} (Ref. 22) and the Si-H related modes at 2000–2150 cm^{-1}.[23] The C-H related stretching modes at 2860–3000 cm^{-1} (Ref. 24) were not distinguishable from the background noise. The peak of the

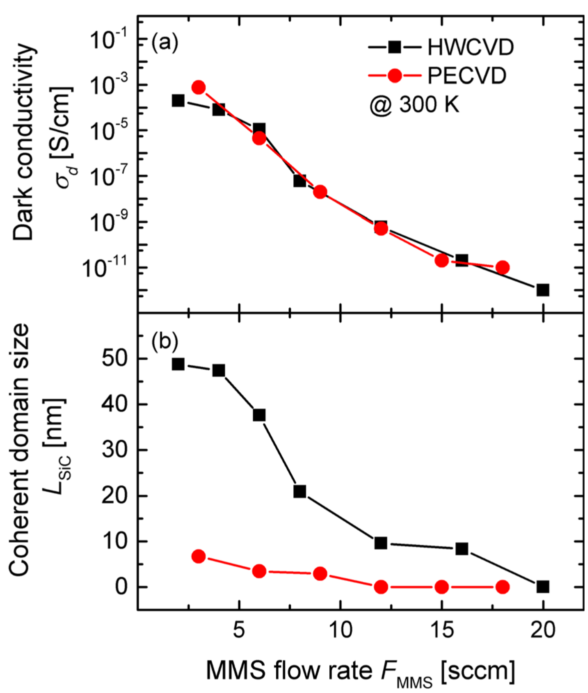

FIG. 1. (a) Electrical dark conductivity σ_d and (b) average coherent domain sizes L_{SiC} derived from XRD measurements of HWCVD (black squares) or PECVD (red circles) grown μc-SiC:H layers where the MMS flow rate was varied $F_{MMS} = 2$–20 sccm and the hydrogen dilution was kept constant.

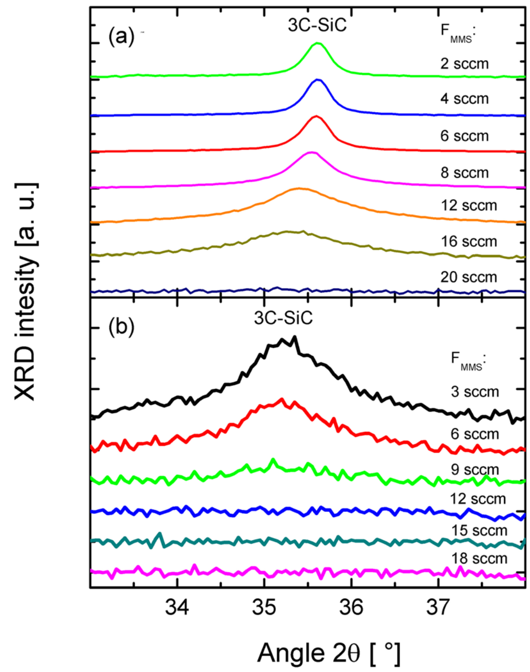

FIG. 2. X-ray diffractograms of (a) HWCVD and (b) PECVD μc-SiC:H films deposited with different MMS flow rates.

Si-C mode is most prominent. For HWCVD layers, the peak intensity decreased from $8.0 \times 10^4\,\mathrm{cm}^{-1}$ to $2.2 \times 10^4\,\mathrm{cm}^{-1}$ and, for PECVD-grown layers, from $3.8 \times 10^4\,\mathrm{cm}^{-1}$ to $1.6 \times 10^4\,\mathrm{cm}^{-1}$, when F_{MMS} was increased. Simultaneously, the FWHM increases for higher F_{MMS} values. For HWCVD layers, it increased from $43.5\,\mathrm{cm}^{-1}$ to $128.3\,\mathrm{cm}^{-1}$ and, for PECVD-grown layers, from $76.7\,\mathrm{cm}^{-1}$ to $156.4\,\mathrm{cm}^{-1}$. In addition, the integrated peak intensity, which is defined as the area below the Si-H related peak, increased with increasing F_{MMS}.

In Fig. 4, the C fraction x, [H], as well [O] and [N] are also plotted as function of σ_d. The [H] was obtained from the Si-H related FTIR modes as reported by King *et al*. All other values were obtained from SIMS measurements.[14] The C fraction decreases for HWCVD layers from $x = 0.49$ for $\sigma_d = 2 \times 10^{-4}$ S/cm to $x = 0.45$ for $\sigma_d = 2 \times 10^{-11}$ S/cm. For HWCVD μc-SiC:H, the [H] increases from $0.4 \times 10^{22}\,\mathrm{cm}^{-3}$ to $1.6 \times 10^{22}\,\mathrm{cm}^{-3}$ for σ_d decreasing from 2×10^{-4} S/cm to 1×10^{-12} S/cm, respectively. For PECVD layers, the C fraction decreases from $x = 0.48$ for $\sigma_d = 8 \times 10^{-4}$ S/cm to $x = 0.40$ for $\sigma_d = 2 \times 10^{-11}$ S/cm. Generally, the [H] in PECVD μc-SiC:H was up to 1.5 times higher. For both deposition techniques, the [O] and [N] did not show any trend over the entire range of σ_d. The values scattered around the following average atomic concentrations: for HWCVD [O] is $5.0 \pm 1.9 \times 10^{19}\,\mathrm{cm}^{-3}$ and [N] is $1.3 \pm 0.6 \times 10^{19}\,\mathrm{cm}^{-3}$, and for PECVD [O] is $1.2 \pm 0.6 \times 10^{21}\,\mathrm{cm}^{-3}$ and [N] is $2.9 \pm 0.4 \times 10^{19}\,\mathrm{cm}^{-3}$.

In Fig. 5, the charge carrier density n as well as the charge carrier mobility μ are plotted as a function of L_{SiC}. For both deposition techniques n strongly increased for larger L_{SiC}. For HWCVD, n increased by 4 orders of magnitude, from $6.8 \times 10^{15}\,\mathrm{cm}^{-3}$ with $L_{\mathrm{SiC}} = 9.6$ nm to $6.2 \times 10^{18}\,\mathrm{cm}^{-3}$ with $L_{\mathrm{SiC}} = 47.4$ nm, whereas μ increases only by less than 1 order of magnitude, namely from 3.2×10^{-5} cm^2/V s to 1.5×10^{-4} cm^2/V s. For PECVD, similar to HWCVD, n increased by 3 orders of magnitude, from $6.7 \times 10^{16}\,\mathrm{cm}^{-3}$

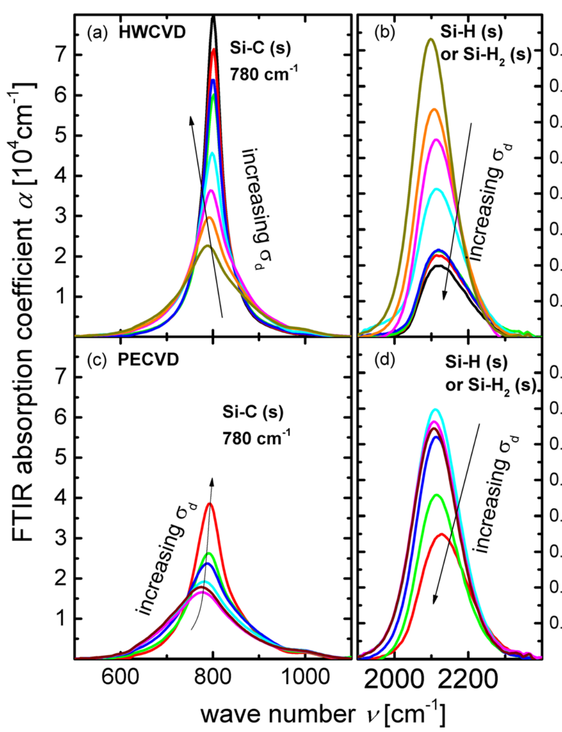

FIG. 3. FTIR modes in μc-SiC:H layers with a very large range of $\sigma_d = 10^{-12}$–10^{-3} S/cm using HWCVD (a) and (b) or PECVD (c) and (d).

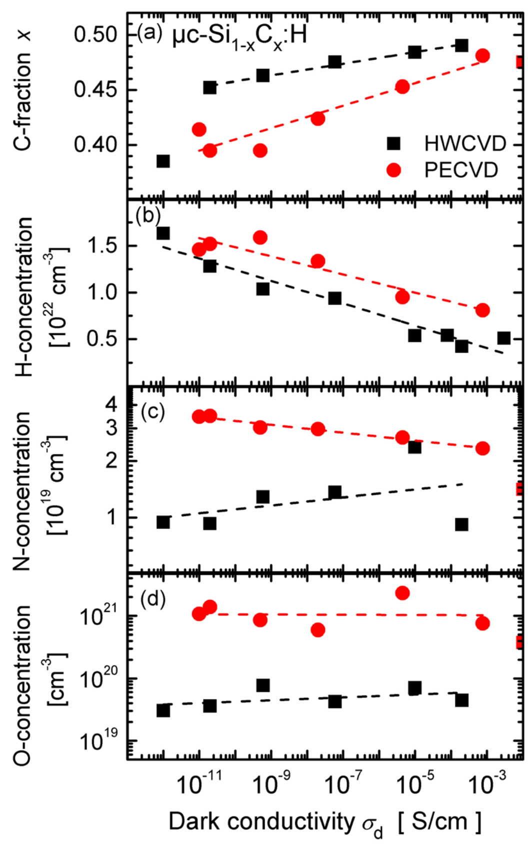

FIG. 4. (a) Carbon fraction x, atomic concentrations of (b) hydrogen, (c) nitrogen, and (d) oxygen for dark conductivities $\sigma_d = 10^{-3}$–10^{-12} S/cm of μc-Si$_{1-x}$C$_x$:H layers deposited by HWCVD (black squares) or PECVD (red circles).

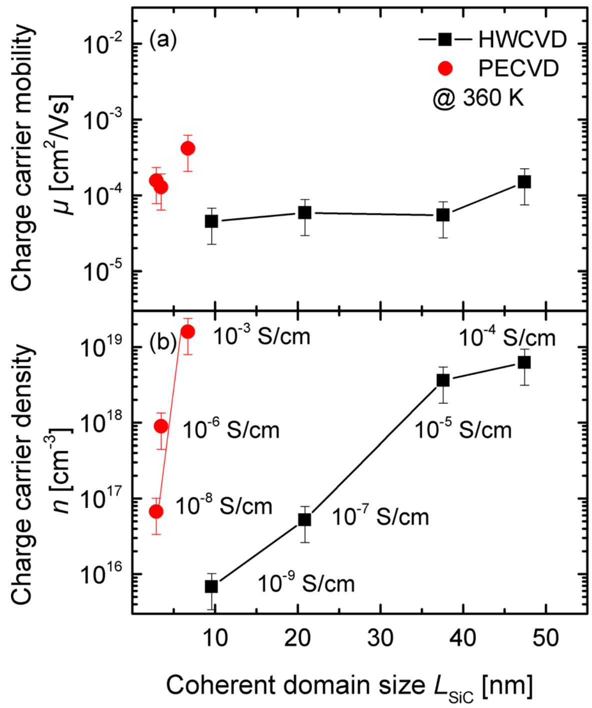

FIG. 5. (a) Charge carrier mobility μ and (b) charge carrier density n of corresponding cubic SiC coherent domain sizes L_{SiC} of μc-SiC:H layers grown by HWCVD (black squares) or PECVD (red circles).

with $L_{SiC} = 2.9$ nm to 1.6×10^{19} cm^{-3} with $L_{SiC} = 6.7$ nm, whereas μ increases only by less than 1 order of magnitude, namely, from 1.3×10^{-4} cm^2/V s to 4.2×10^{-4} cm^2/V s. The values of the thermo-voltage (not shown) decreased from $-1200\,\mu$V/K to $-560\,\mu$V/K for increasing L_{SiC}.

In Fig. 6, the activation energy of the dark conductivity E_a, of the mobility μ_T and of charge carrier density n_T are plotted as a function of L_{SiC}. For HWCVD films, E_a decreases from 0.51 eV to 0.19 eV for increasing L_{SiC} from 9.6 nm to 47.4 nm. Similarly, also μ_T and n_T decrease from 0.33 eV to 0.14 eV and from 0.18 eV to 0.04 eV, respectively.

IV. DISCUSSION

The values for dark conductivity σ_d of the HWCVD and the PECVD μc-SiC:H layers cover a large range, namely,

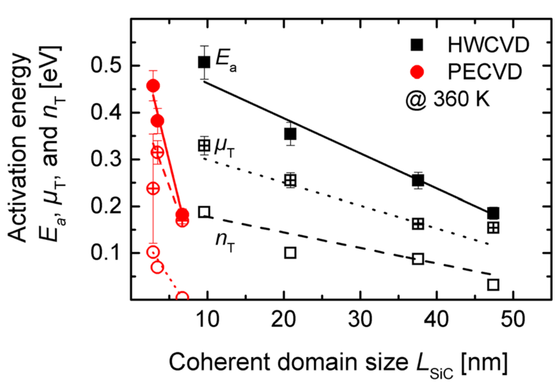

FIG. 6. Activation energy of dark conductivity E_a (filled symbols), of mobility μ_T (symbols with cross), and of charge carrier density n_T (empty symbols) of corresponding cubic SiC coherent domain sizes L_{SiC} of μc-SiC:H layers grown by HWCVD (black squares) or PECVD (red circles).

2.0×10^{-4}–1×10^{-12} S/cm, offering the opportunity to relate the μc-SiC:H material structure and its impurities to the general electrical transport mechanisms.

In order to produce layers with conductivities of this very large range, we varied the monomethylsilane flow rate F_{MMS}, while keeping the hydrogen dilution and all other parameters constant or in other words, we varied the total gas flow rate. Evolution of microstructure and electronic properties in growth direction is commonly observed in disordered semiconductor films deposited of gas phase. In order to minimize a possible impact of the film thickness we adjusted the deposition time to obtain a thickness of approximately 200 nm for all samples in the study. The influence of F_{MMS} on the material properties is comparable with the influence of an increase of hydrogen dilution, as reported by Finger *et al.*[2] and Miyajima *et al.*[6] They conclude that an increase of hydrogen dilution leads to a decrease of disorder in the microstructure. Similarly, we derived from the FWHM of the FTIR and XRD data that the reduction of F_{MMS} leads to a decrease of disorder in the microstructure. From the shift of the SiC peak position in FTIR and in XRD we derive that the binding length of Si-C decreases when F_{MMS} is reduced. In addition to the higher order in the microstructure, we also observe an approach of C-fraction x closer to 0.5, an increase of the coherent domain size L_{SiC}, and a decrease of hydrogen concentration [H] for both deposition methods. The variation of all these material parameters seems to play an important role for an improvement of σ_d, if no active doping gas is used. It seems that using smaller F_{MMS} or, in other words, providing a longer residence time per MMS-molecule, permits all Si and C atoms to find an energetically better position on the substrate surface.

It has been suggested by Refs. 2 and 6 that a deposition from MMS gas as precursor would be beneficial for the formation of perfectly stoichiometric μc-Si$_{1-x}$C$_x$:H layers with $x = 0.5$, as MMS (CH_3SiH_3) contains Si and C in equal proportions. Nevertheless, our SIMS measurements reveal an Si excess for all samples, even though MMS was used for the formation of μc-SiC:H. According to Köhler *et al.*[12] and according to the measured XRD data obtained from the present series, there is no amorphous phase detected for μc-SiC:H. Hence, the question about the location of the excess silicon arises. SiC coherent domains are expected to be stoichiometric. Therefore, the excess silicon has to be located outside of the domains bulk. Here we propose a hypothesis to resolve this discrepancy. If we assume all SiC coherent domain surfaces to be Si-terminated, it would lead to higher Si content, if a large number of small coherent domains come into play. The validity of this assumption can be checked with a simple estimation. We quantify the theoretical amount of Si atoms, hypothetically located at SiC coherent domain surfaces, and compare it with the measured values of excess Si. To do so, we simplify the form of the SiC coherent domains to cubes with a size of L. The thickness of a crystalline SiC monolayer is given by $D^{-1/3}$, where D is the crystalline SiC density (9.68×10^{22} cm^{-3} (Ref. 25)). Therefore, the volume of the coherent domain surface layer V_s of a single cubic monocrystal can be written as

$$V_s = 6L^2 D^{-1/3}. \quad (2)$$

By definition, the surface layer consists of equal quantity of Si and C atoms. Assuming that the coherent domains are completely Si-terminated, then leads to the fact, that all C atoms of the surface layer would be replaced by Si atoms, which would use an approximate volume of $V_s/2$. It is also possible to express the volume of the Si excess as $(1–2x)L^3$. By combining both equations as $(1–2x)L^3 = V_s/2 = 3L^2D^{-1/3}$, the coherent domain size L can be written as

$$L(x) = \frac{3D^{-\frac{1}{3}}}{(1-2x)}. \quad (3)$$

This relation is plotted in Fig. 7 together with our experimental data of L_{SiC} and C fraction x of HWCVD and PECVD layers. The calculated curve from Eq. (3) is in good agreement with our experimental data. Therefore, we propose that the SiC coherent domains could be terminated by the excess silicon.

Before the Si-termination can be related to the electrical properties of μc-SiC:H, it is also important to discuss the location of H. Since the solubility of H in crystalline SiC (c-SiC) is very low ($10^{14}\,cm^{-3}$ (Ref. 26)), we propose that most of H atoms should be situated outside the SiC coherent domains. As further the material seems to not contain an amorphous phase,[12] we suggest that H atoms should be mostly bound to the Si atoms that terminate the surfaces of the SiC coherent domains. In order to examine the validity of this suggestion, the concentration of Si at the coherent domain surfaces can be compared with the determined H concentration of the films. From $(1–2x)$D we can derive the Si excess concentration at coherent domain surfaces for all C-fractions x and compare it with the corresponding [H], as shown in Fig. 8. In average, we find a $2.8 \times 10^{21}\,cm^{-3}$ higher concentration of H than Si-excess for HWCVD layers. For PECVD, [H] seems to depend also linearly on Si-excess concentration. Thus, we can only speculate that H could be partially located at the SiC coherent domain surfaces. Another aspect of μc-SiC:H films is the presence of an amorphous nucleation zone, where all the other H atoms could be located. The μc-SiC:H films are probably sufficiently thick,

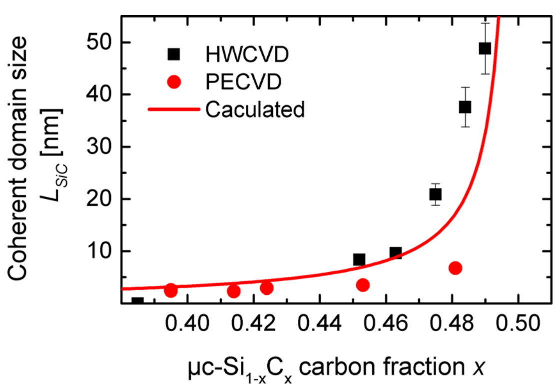

FIG. 7. Cubic SiC coherent domain sizes L_{SiC} are correlated with carbon fraction x of layers grown by HWCVD (black squares) and PECVD (red circles). Additionally, calculated $L_{SiC} = 6/2\ D^{-1/3}(1–2x)^{-1}$ is also plotted, where D is the crystalline SiC density ($9.68 \times 10^{22}\,cm^{-3}$ (Ref. 25)).

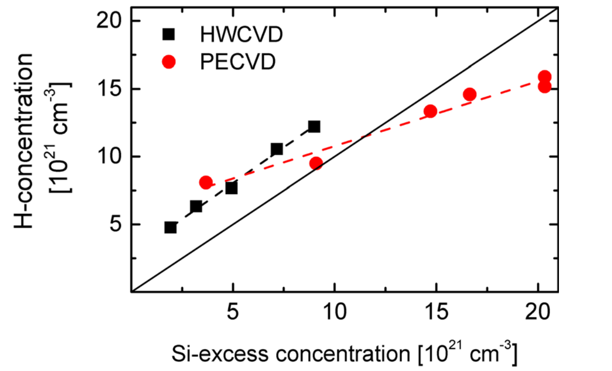

FIG. 8. Hydrogen concentration, derived from FTIR measurements, as a function of silicon excess concentration, derived from SIMS measurements in HWCVD (black squares) and PECVD (red circles) grown μc-SiC:H layers.

so that the amorphous nucleation zone could not be sufficiently detected by our XRD measurements, which should also be valid for the XRD data published by Köhler *et al.*[12] Qualitatively, our idea of H being located in amorphous phases between the coherent domains and in the nucleation zone would be in good agreement with the work of Heidt *et al.*[27] who observed a high degree of disorder within the nucleation zone and at heterogeneous grain boundaries, by using energy filtered transmission electron microscopy.

Following our hypothetical model that larger coherent domain sizes might lead to smaller SiH_x termination concentrations, the question arises, whether a decrease in termination concentration is the origin for the improvement of the electrical transport in the material. In Fig. 4(b), for both deposition techniques σ_d increases drastically with decreasing [H]. However, it is difficult to draw a direct relation between the decrease of SiH_x termination concentration and the increase in n by 4 orders of magnitude that we observed (Fig. 5), while μ only increases by less than 1 order of magnitude. In the literature, O and N impurities originating from contamination are discussed as possible candidates for the creation of donor-like states within the energy gap of μc-SiC:H.[2,6,7] From c-SiC it is well known that N is a very good shallow donor impurity, due to its low ionization energy.[28] Unlike the case of unintentionally n-type doped microcrystalline silicon, where the use of gas purifiers during deposition decreased [O] and σ_d,[29] Finger *et al.*[2] reported that the electrical properties of unintentionally n-type doped μc-SiC:H were not affected by gas purifiers. In the present work, although σ_d covers a very large range—9 orders of magnitude—[O] and [N] remain constantly high at the order of magnitude of $10^{19}\,cm^{-3}$ (Figs. 4(c) and 4(d)), so that it is not possible to derive a direct correlation between [O] and σ_d, or [N] and σ_d. In the following we discuss two plausible options that might explain the strong increase of σ_d, which is dominated by an increase of n, without any increase of the donor impurity concentrations.

A plausible option could be a H passivation of the donors, as reported by several groups for c-SiC.[30–32] The groups calculated the passivation level from the drop in electron spin resonance (ESR) signal for nitrogen-related paramagnetic states before and after hydrogenation of the c-SiC, and crosschecked it by measuring n. Qualitatively, the decrease in [H] for increasing n, while [N] and also [O] remain constant, would be in good agreement with the idea of donor passivation by H. To verify or exclude H passivation of donor impurities, extensive ESR study is necessary in the future.

Another plausible option to explain the strong increase of charge carrier density n arises from the Seto model.[33] Seto assumed a doped polycrystalline silicon material composed of grains of identical size and differentiated between bulk region and grain boundary region. The bulk region can be treated as crystalline silicon whereas the regions of the grain boundaries contain trap states in the band gap. Consequently, in the bulk the position of the Fermi level is defined by donor or acceptor states and at the boundary by trap states that cause a depletion of that region. Following the model of Seto, we can try to explain the dependence of n and L_{SiC}. According to the model, the average carrier concentration n in a grain should consist of contributions from the depleted grain boundary region and the undepleted bulk of the grain. Thus, for small grains, the depletion region would cause a reduction of the average n in the grain, whereas for larger grains the effect of the depleted grain boundaries should be smaller, which is qualitatively in good agreement with our results (Fig. 5(b)). In addition, the reduction of the activation energy E_{a} for larger L_{SiC}, shown in Fig. 6, is consistent with the introduced idea, as it can be considered as an integrated value of all local activation energies from one coherent domain boundary to the other. In addition, the thermal activation of mobility μ_{T} and thermal activation of charge carrier density n_{T} also support the proposed idea as they also decrease for larger coherent domains (Fig. 6). Based on Seto's model

$$\mu \propto L \exp\left(-\frac{E_B}{k_B T}\right), \tag{4}$$

where L is the coherent domain size, E_{B} the barrier potential height, and T the temperature. Assuming E_{B} to be constant for different L_{SiC} in our case, qualitatively the trend for $\mu(L)$ (Fig. 5(a)) is not in contradiction with Seto's model.

Finally, it might seem contradictory that on the one hand σ_{d} and n show such a strong dependence on L_{SiC} (Figs. 1 and 5(b)), but are similar for both techniques, although L_{SiC} is very different. For instance, the HWCVD layer with $L_{\mathrm{SiC}} = 8$ nm only shows $\sigma_{\mathrm{d}} = 10^{-11}$ S/cm whereas the PECVD layer with $L_{\mathrm{SiC}} = 7$ nm provides $\sigma_{\mathrm{d}} = 10^{-3}$ S/cm. Probably a major reason is that all electrical transport properties, i.e., σ_{d}, n, and μ, are measured in plane to the growth direction whereas L_{SiC}, derived from XRD, represents the average coherent domain size perpendicular to the growth direction. From literature it is known that HWCVD SiC grains grow in the form of columns along the film growth,[2,12,27] whereas PECVD SiC grains grow in the form of well-distributed ellipsoids.[34] Hence, it would be possible that for same σ_{d} the corresponding lateral coherent domain sizes are similar for both deposition methods. Another aspect is the huge difference in [O] for both layer types. For all HWCVD layers the [O] is in average $5.0 \pm 1.9 \times 10^{19}\,\mathrm{cm}^{-3}$, whereas for all PECVD layers the [O] is in average $1.2 \pm 0.6 \times 10^{21}\,\mathrm{cm}^{-3}$. The effect and the origin of very high [O] in μc-SiC:H are not yet understood and require more investigations in the future. Moreover, it remains unclear if N or O impurities—or both—are responsible for electrical transport in unintentionally n-type μc-SiC:H.

V. CONCLUSION

In this work, we present new insight into the microstructure of unintentionally n-type doped μc-SiC:H thin-films and the understanding of the mechanisms responsible for their unique electrical properties if no active doping gas was used during the HWCVD or PECVD fabrication. We found out by SIMS measurements that no direct correlation exists between oxygen or nitrogen concentrations and high dark conductivity σ_{d}, high charge carrier density n, and low activation energy E_{a}. Higher σ_{d} seems to rise from lower hydrogen concentrations or/and larger coherent domain sizes L_{SiC}. On the one hand, the decrease of σ_{d} with increasing hydrogen concentration might be due to the inactivation of donors by hydrogen passivation that gives rise to decreased n. On the other hand, qualitatively consistent with the Seto model, the lower σ_{d} and lower n might be caused by smaller L_{SiC}, since the fraction of depleted grain boundaries with higher E_{a} increases accordingly.

ACKNOWLEDGMENTS

We would like to thank S. Lynen and M. Meyer for FTIR and dark conductivity measurements. We like to thank J. Wolff and A. Schmalen for fruitful discussions and technical support.

[1] T. Chen, F. Köhler, A. Heidt, R. Carius, and F. Finger, "Hot-wire chemical vapor deposition prepared aluminum doped p-type microcrystalline silicon carbide window layers for thin film silicon solar cells," Jpn. J. Appl. Phys., Part 1 **53**(5S1), 05FM04 (2014).

[2] F. Finger, O. Astakhov, T. Bronger, R. Carius, T. Chen, A. Dasgupta, A. Gordijn, L. Houben, Y. Huang, S. Klein, M. Luysberg, H. Wang, and L. Xiao, "Microcrystalline silicon carbide alloys prepared with HWCVD as highly transparent and conductive window layers for thin film solar cells," Thin Solid Films **517**(12), 3507–3512 (2009).

[3] M. Pomaska, W. Beyer, E. Neumann, F. Finger, and K. Ding, "Impact of microcrystalline silicon carbide growth using hot-wire chemical vapor deposition on crystalline silicon surface passivation," Thin Solid Films **595**, 217–220 (2015).

[4] J. Irikawa, S. Miyajima, T. Watahiki, and M. Konagai, "High efficiency hydrogenated nanocrystalline cubic silicon carbide/crystalline silicon heterojunction solar cells using an optimized buffer layer," Appl. Phys. Express **4**(9), 092301 (2011).

[5] H. Matsumura and K. Ohdaira, "Cat-CVD (Catalytic-CVD): Its fundamentals and application," ECS Trans. **25**(8), 53–63 (2009).

[6] S. Miyajima, A. Yamada, and M. Konagai, "Characterization of undoped, n- and p-type hydrogenated nanocrystalline silicon carbide films deposited by hot-wire chemical vapor deposition at low temperatures," Jpn. J. Appl. Phys., Part 1 **46**(4A), 1415–1426 (2007).

[7] S. Klein, A. Dasgupta, F. Finger, R. Carius, and T. Bronger, "Electronic properties of low temperature microcrystalline silicon carbide prepared by hot wire CVD," Thin Solid Films **516**(5), 630–632 (2008).

[8] A. Tabata, Y. Hoshide, and A. Kondo, "Highly conductive nitrogen-doped hydrogenated nanocrystalline cubic silicon carbide thin films prepared with a hot-wire chemical vapor deposition from $SiH_4/CH_4/H_2/N_2$ gas," Mater. Sci. Eng. B **175**(3), 201–206 (2010).

[9]S. Miyajima, A. Yamada, and M. Konagai, "Aluminum-doped hydrogenated microcrystalline cubic silicon carbide films deposited by hot wire CVD," Thin Solid Films **501**(1–2), 186–189 (2006).

[10]T. Chen, D. Yang, R. Carius, and F. Finger, "Aluminum doped silicon carbide thin films prepared by hot-wire CVD: Influence of the substrate temperature on material properties," Thin Solid Films **519**(14), 4516–4518 (2011).

[11]F. Demichelis, C. F. Pirri, E. Tresso, and P. Rava, "Doped amorphous and microcrystalline silicon carbide as wide band-gap material," in *Wide Band Gap Semiconductors* (Materials Research Society, 1992), Vol. 242, pp. 675–680.

[12]F. Köhler, T. Chen, M. Nuys, A. Heidt, M. Luysberg, F. Finger, and R. Carius, "Microstructure of hydrogenated silicon carbide thin films prepared by chemical vapour deposition techniques," J. Non-Cryst. Solids **358**(17), 2011–2014 (2012).

[13]J. I. Langford and A. J. C. Wilson, "Scherrer after sixty years: A survey and some new results in the determination of crystallite size," J. Appl. Crystallogr. **11**(2), 102–113 (1978).

[14]S. W. King, J. Bielefeld, M. French, and W. A. Lanford, "Mass and bond density measurements for PECVD a-SiCx:H thin films using Fourier transform-infrared spectroscopy," J. Non-Cryst. Solids **357**(21), 3602–3615 (2011).

[15]R. G. Wilson, F. A. Stevie, and C. W. Magee, *Secondary Ion Mass Spectrometry—A practical Handbook for Depth Profiling and Bulk Impurity Analysis* (John Wiley & Sons, 1989), p. 3.1–1.

[16]Y. Gao, "A new secondary ion mass spectrometry technique for III-V semiconductor compounds using the molecular ions CsM+," J. Appl. Phys. **64**(7), 3760–3762 (1988).

[17]H. Gnaser, "Improved quantification in secondary-ion mass spectrometry detecting MCs+ molecular ions," J. Vac. Sci. Technol. A **12**(2), 452–456 (1994).

[18]F. Caccavale, G. Brusatin, and I. Kleps, "A combined use of SIMS and RBS techniques for the investigation of SiC and SiCN films," Appl. Surf. Sci. **81**(4), 443–447 (1994).

[19]W. Beyer and H. Overhof, "Doping effects in a-Si: H," in *Semiconductors and Semimetals*, edited by J. I. Pankove (Elsevier, 1984), Vol. 21, Part C, Chap. 8, pp. 257–307.

[20]R. A. Street, "Electronic transport," in *Hydrogenated Amorphous Silicon* (Cambridge University Press, Cambridge, 1991), pp. 224–275.

[21]C. Sellmer and U. Rau, *Untersuchung der Ladungsträgerkonzentration und -beweglichkeit in mikrokristallinen Siliziumlegierungen mit Hall-Effekt und Thermokraft 2011-09-27* (Publikationsserver der RWTH Aachen University, 2011).

[22]L. Calcagno, F. Giorgis, A. Makthari, P. Musumeci, and F. Pirri, "Compositional and structural properties of deuterated plasma enhanced chemical vapour deposited silicon-carbon alloys," Philos. Mag. Part B **79**(10), 1685–1694 (1999).

[23]M. Cardona, "Vibrational Spectra of Hydrogen in Silicon and Germanium," Phys. Status Solidi B **118**(2), 463–481 (1983).

[24]F. Demichelis and C. F. Pirri, "Hydrogenated amorphous silicon based alloy: A-Si_{1-x}C_x:H," Solid State Phenom. **44–46**, 385–424 (1995).

[25]R. G. Wilson, F. A. Stevie, and C. W. Magee, "Appendix," in *Secondary Ion Mass Spectrometry* (John Wiley & Sons, USA, 1989), p. App. C.3.

[26]R. A. Causey, J. D. Fowler, C. Ravanbakht, T. S. Elleman, and K. Verghese, "Hydrogen diffusion and solubility in silicon carbide," J. Am. Ceram. Soc. **61**(5–6), 221–225 (1978).

[27]A. Heidt, T. Chen, R. Carius, F. Finger, U. Rau, J. Mayer, and M. Luysberg, "Structure and electronic properties of μc-SiC:H for photovoltaic applications," J. Phys. Conf. Ser. **326**(1), 012019 (2011).

[28]H.-J. Rost, D. Schulz, and D. Siche, "High nitrogen doping during bulk growth," in *Silicon Carbide Recent Major Advances* (Springer, 2004), pp. 163–178.

[29]P. Torres, J. Meier, R. Flückiger, U. Kroll, J. A. A. Selvan, H. Keppner, A. Shah, S. D. Littelwood, I. E. Kelly, and P. Giannoulès, "Device grade microcrystalline silicon owing to reduced oxygen contamination," Appl. Phys. Lett. **69**(10), 1373–1375 (1996).

[30]F. Gendron, L. M. Porter, C. Porte, and E. Bringuier, "Hydrogen passivation of donors and acceptors in SiC," Appl. Phys. Lett. **67**(9), 1253–1255 (1995).

[31]A. Gali, P. Deák, N. T. Son, and E. Janzén, "Hydrogen passivation of nitrogen in SiC," Appl. Phys. Lett. **83**(7), 1385–1387 (2003).

[32]P. Deák, A. Gali, and B. Araadi, "Hydrogen in SiC," in *Silicon Carbide Recent Major Advances* (Springer, 2004), pp. 57–88.

[33]J. Y. W. Seto, "The electrical properties of polycrystalline silicon films," J. Appl. Phys. **46**(12), 5247–5254 (1975).

[34]S. Miyajima, M. Sawamura, A. Yamada, and M. Konagai, "Effects of hydrogen dilution ratio on properties of hydrogenated nanocrystalline cubic silicon carbide films deposited by very high-frequency plasma-enhanced chemical vapor deposition," Jpn. J. Appl. Phys., Part 2 **46**(7L), L693 (2007).